On sound production from the interaction of two planar flames

M. Talei[1], M. J. Brear[1] and E. R. Hawkes[2]

[1] Department of Mechanical Engineering, University of Melbourne, Victoria, Australia

[2] School of Photovoltaic and Renewable Energy Engineering/School of Mechanical and Manufacturing Engineering,
University of New South Wales, Sydney, Australia

Abstract

This paper presents a numerical and theoretical investigation of the sound generated by planar premixed flame annihilation. The compressible Navier-Stokes, energy, and progress variable equations are first solved using Direct Numerical Simulation (DNS), resolving both the flame dynamics and the acoustics. These simulations show that the amplitude of the far-field sound produced by the planar annihilation events depends on the laminar flame speed and temperature ratio.

A theory is then presented that relates the far-field sound to the flame annihilation event by using a previously reported and extended form of Lighthill's acoustic analogy. A comparison with the numerical results shows that this theory accurately represents the far-field sound produced by considering only the temporal heat release source term in Lighthill's acoustic analogy, as reported by others. Additional assumptions of an infinitely thin flame and constant flame speed are then invoked in an attempt to simplify the problem. This theory results in good predictions of the overall pressure change.

Introduction

Combustion is a significant source of noise pollution. Combustion generated sound also plays a central role in the stability of many engineering devices such as industrial burners, gas turbines and rockets [e.g. 7, 1]. The ongoing pursuit of quieter and cleaner combustion in these devices provides a continued need for further refinements in our understanding of combustion generated sound.

Strahle [10] constructed a theory of combustion noise by extending Lighthill's acoustic analogy [8] to combusting flows. Under the assumptions of low Mach number and a constant average mixture molecular weight, Lighthill's acoustic analogy can be simplified to an inhomogeneous wave equation with a single monopolar source term [11, 4]. This source term has been written in terms of time derivatives of the heat release rate or the flame volume.

One mechanism affecting the flame volume, and hence sound generation, is flame annihilation [6, 2]. For example, when two flame surfaces interact the unburnt gas trapped between these surfaces is consumed, resulting in a rapid reduction in flame surface area and thus heat release. Candel et al [2] studied sound generation by mutual flame annihilation and concluded that the dominant mechanism of sound generation was flame surface destruction.

The aims of this study is therefore to investigate the mechanism of sound generation by the collision of planar premixed flames using DNS. Simple chemistry is used since the dependence of radiated sound on even basic parameters such as the flame thickness is not yet established. A theory is then developed for these cases using an extended form of Lighthill's equation [4]. Key parameters are subsequently identified and their influence on the far-field sound is investigated further.

Numerical Methods and Flow Parameters

The Direct Numerical Simulation of sound generated by a premixed flame is a challenge. Care must be taken to simultaneously ensure adequate resolution of the flame, whilst providing a large enough computational domain to resolve the larger long-wavelengths of the radiated sound. These requirements were achieved in the present study by using the code NTmix featuring a 6th order compact scheme for spatial derivatives, combined with a 3rd order Runge-Kutta time integrator [3].

The governing equations were discretised into 3000 nodes from $x = 0$ to $15L_{ref}$, where L_{ref} is the reference length. There were at least 10 grid points inside the flame thickness at all times. A symmetry boundary condition was used to simulate half of the domain. The outflow boundaries were modelled with non-reflecting boundary conditions [9]. The Zeldovich number is 8 and the Prandtl number is 0.75 for all simulations.

In all simulations, the flow field is initialised with a region of unbunt gas from $x = 0$ to $x = 7.5L_{ref}$ that is surrounded by burnt gas from $x = 7.5L_{ref}$ to $x = 15L_{ref}$ at the adiabatic flame temperature. After initialising the flow field the flame starts to propagate towards the origin. The propagation velocity is initially equal to the planar laminar flame speed but varies as the flame approaches the symmetry plane. Three cases of different flame thicknesses ($\delta/L_{ref} = 0.1, 0.2$ and 0.4) have been studied.

Numerical Results

Consider case 1 ($\delta/L_{ref} = 0.1$) as the baseline case. The top frame in Figure 1 shows the reaction rate normalised by its value in the far field $\dot{\omega}/(\dot{\omega}_{max})_\infty$ versus normalised distance x/δ at several instants. The flame propagates from right to left and the symmetry plane is at $x/\delta = 0$. It may be observed that the reaction rate retains close to the same spatial profile throughout. Once the flame is close to the symmetry plane, the reaction rate starts to increase marginally. Finally, as the reactants are progressively consumed, the peak reaction rate decreases until the flame is annihilated. Figure 1ii shows the reduced temperature $\Theta = (T - T_u)/(T_b - T_u)$ versus normalised distance for several instants. The variable T is the temperature and the subscripts b and u refer to burnt and unburnt gas respectively. As can be seen the reduced temperature increases as two preheat zones start to merge. After the extinction event, the temperature is uniform and equal to the burnt gas temperature throughout the domain.

Now consider the pressure, which is shown in the bottom frame of Figure 1. The variable p is the pressure, ρ is the density and c is the sonic velocity. Before the annihilation event there is small change in the pressure profile across the flame corresponding to the pressure gradient required to accelerate the unburned gases to the positive burned gas velocity. However, during the extinction event, the pressure at the origin first increases then decreases, leading to a much larger pressure pulse that propagates away from the symmetry plane in the positive x-direction.

The propagating sound wave resulting from flame annihilation
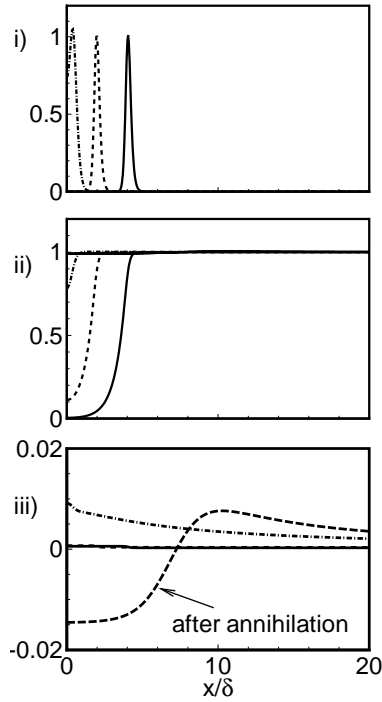
Figure 1: i) Non-dimensional reaction rate $\dot{\omega}/(\dot{\omega}_{max})_\infty$, ii) reduced temperature Θ, and iii) non-dimensional pressure $(p - p_{ref})/\rho_{ref} c_{ref}^2$ versus distance from the origin non-dimensionalised by flame thickness δ at different instants before (solid), during (dashed and dash-dot) and after (long dash) annihilation.

may be observed in an $x-t$ diagram (Figure 2). Here, the time $t = 0$ refers to the instant when the point of maximum reaction rate reaches the symmetry plane. At negative times (prior to collision), the nearly vertical contour lines reflect the slow propagation of the laminar flame. During the annihilation event acoustic energy is produced. The sound wave resulting from flame annihilation then appears as a pressure wave moving towards the outflow boundaries at the sonic velocity of the burnt gas, as evidenced by the diagonal contour lines in the $x-t$ diagram.

Figure 3 shows a comparison between a temporal history of pressure observed near the origin and in the far-field. As can be seen there is a maxima in the pressure history which will be termed the 'peak pressure'. The generated pressure wave after the annihilation event has a steady state value that is less than the reference pressure. This pressure will be referred to as the steady state far-field pressure in Figure 3. Note that the pressure in the far-field has a very similar temporal history to that at the origin.

Figure 4 shows a comparison of pressure versus time at two points in the domain for each of the different flame thicknesses. Figure 4i shows the pressure at a point near the annihilation location ($\zeta/L_{ref} = 0$) while Figure 4ii) shows a point in the far-field ($\zeta/L_{ref} = 7.5$) for all flame thicknesses. Flame thickness can be seen to have negligible effect on the peak pressure. The steady state far-field pressure does not vary as the flame thickness is changed both at the symmetry plane and in the far-field.

Theoretical Analysis

In order to investigate further the mechanism of sound gener-
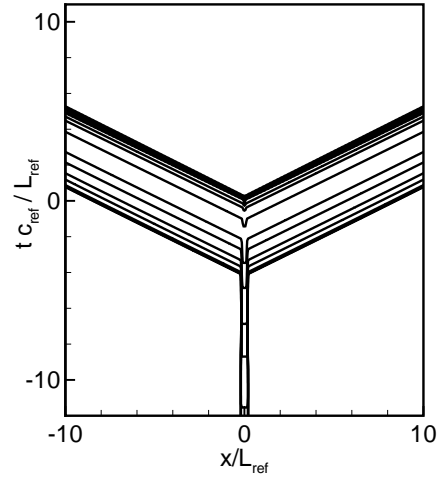
Figure 2: $x-t$ diagram of the pressure field during the collision of two planar flames.
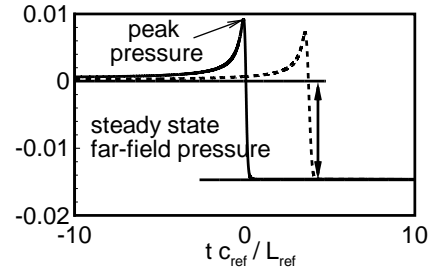
Figure 3: Non-dimensional pressure $(p - p_{ref})/\rho_{ref} c_{ref}^2$ for flame annihilation from DNS at the symmetry axis (solid line) and in the far-field $x/L_{ref} = 7.5$ (dashed line).
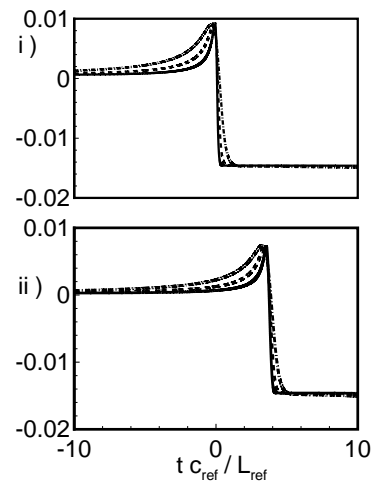
Figure 4: Non-dimensional pressure $(p - p_{ref})/\rho_{ref} c_{ref}^2$ for flame annihilation from DNS i) at the symmetry axis and ii) in the far-field $x/L_{ref} = 7.5$ for different flame thicknesses, solid line: $\delta/L_{ref} = 0.1$, dashed: $\delta/L_{ref} = 0.2$, dash-dot: $\delta/L_{ref} = 0.4$
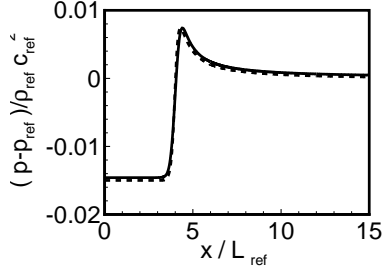
Figure 5: Non-dimensional pressure $(p - p_{ref})/\rho_{ref} c_{ref}^2$ from i) DNS, solid line, ii) solution of equation 1, $\delta/L_{ref} = 0.1$.

ation, a theory is now developed to describe the production of sound as a function of key flame parameters. By retaining only the source term associated with temporal fluctuations in the heat release and under the assumption of low Mach number, Dowling's rearranged form of Lighthill's equation can be expressed as,

$$\frac{1}{c_\infty^2}\frac{\partial^2 p}{\partial t^2} - \nabla^2 p = \left(1 - \frac{T_u}{T_b}\right)\frac{\partial}{\partial t}\left(\dot{\omega}(r,t)\right). \quad (1)$$

The solution can be obtained using a free-space Green's function [e.g. 5],

$$p'(r,t) = p(r,t) - p_{ref}$$
$$= \left(1 - \frac{T_u}{T_b}\right)\int_0^{t^+}\iiint_{V_0} G(r,t|r_0,\tau)\frac{\partial}{\partial\tau}\left(\dot{\omega}(r_0,\tau)\right)dV_0 d\tau, \quad (2)$$

where r is the position vector for any point inside or outside the source region, r_0 is the position vector in the source region, V_0 is the volume of the source region and t^+ denotes the time slightly later than t and $\tau \in [0, t^+]$. The Green's function $G(r,t|r_0,\tau)$ is as follows,

$$\frac{c_\infty}{2}H(t - \tau - \frac{|r - r_0|}{c_\infty}).$$

To evaluate the theoretical assumptions up to this point, Figure 5 shows a comparison of DNS with the solution of Lighthill's equation retaining only the heat release term (equation 1). The graphs show pressure at an instant after annihilation. There is a very good agreement between theory and simulation which shows that considering the heat release term as the main mechanism of sound generation is a reasonable assumption. Given the rate of reaction, equation 2 provide a means of determining sound production. In the ensuing sections, particular results for each configuration are now developed under increasingly restrictive assumptions.

Flames of finite thickness

Recall that Figure 1 showed that the spatial variations of reaction rate relative to flame location were fairly time invariant. The reaction rate may therefore be modelled by taking the spatial dependence to be a temporally invariant function f,

$$\dot{\omega} = f(\zeta_f(\tau) - |\zeta|), \quad (3)$$

where $\zeta_f(\tau)$ represents the instantaneous location of the flame and can be defined as the location of maxima in the reaction rate profile. The variable ζ is the axial coordinate. For a flame which is far from the centre of the domain,

$$\int_0^{+\infty} f(\zeta_f - |\zeta|)d\zeta = \rho_u S_L, \quad (4)$$

where S_L is the laminar flame speed. Using the Green's function solution of equation 1, the pressure may be obtained in the far-field:

$$p'(x,t) = \frac{c_b}{2}\left(1 - \frac{T_u}{T_b}\right)\int_{-\zeta^+}^{+\zeta^+}\int_0^{t - \frac{|x-\zeta|}{c_b}}\frac{\partial\dot{\omega}}{\partial\tau}d\zeta d\tau,$$
$$= \frac{c_b}{2}\left(1 - \frac{T_u}{T_b}\right)\int_{-\zeta^+}^{+\zeta^+}\dot{\omega}(\zeta, t - \frac{|x - \zeta|}{c_b})d\zeta$$
$$- \frac{c_b}{2}\left(1 - \frac{T_u}{T_b}\right)\int_{-\zeta^+}^{+\zeta^+}\dot{\omega}(\zeta, 0)d\zeta, \quad (5)$$

where ζ^+ specifies the size of the source region. The second integral term on the right hand side of equation 5 is proportional to the integral of the reaction rate of the two flames before the collision event and can be obtained using equation 4,

$$\frac{c_b}{2}\left(1 - \frac{T_u}{T_b}\right)\int_{-\zeta^+}^{+\zeta^+}\dot{\omega}(\zeta, 0)d\zeta = \rho_u c_b\left(1 - \frac{T_u}{T_b}\right)S_L. \quad (6)$$

The evaluation of the first integral term on the right hand side of equation 5 can be done by assuming that $|x| \longrightarrow \infty$ and so $|x - \zeta| \approx |x|$. If τ_1 is defined as the instant that the total integrated reaction rate starts to change when the flame is close to the origin (recall Figure 1) and τ_2 as the instant at which the flame has just disappeared, the first integral term in equation 5 can be obtained to express the final solution,

$$p'(x,t) =$$
$$\begin{cases} 0 & t - |x|/c_b < \tau_1 \\ \rho_u c_b\left(1 - \frac{T_u}{T_b}\right)S_L\left(\frac{\dot{\omega}_T(t - |x|/c_b)}{\rho_u S_L} - 1\right) & \tau_1 < t - |x|/c_b < \tau_2 \\ -\rho_u c_b\left(1 - \frac{T_u}{T_b}\right)S_L & \tau_2 < t - |x|/c_b \end{cases}$$
$$(7)$$

where $\dot{\omega}_T$ is the instantaneous total reaction rate (*i.e.* the reaction rate integrated over space). Equation 7 has three parts. The first part of the solution $(t - |x|/c_b < \tau_1)$ shows that the net sound production where the flame is reasonably far from the symmetry plane is zero, as expected. The second part $(\tau_1 < t - |x|/c_b < \tau_2)$ corresponds to when the annihilation event occurs and the total reaction rate starts to change. In the last term $(\tau_2 < t - |x|/c_b)$ the sound produced as a result of complete annihilation appears as a constant negative pressure wave. This instant is when the acoustic wave produced during collision has passed the observer located at x, resulting in the steady state far-field pressure. The theory therefore suggests that the steady state pressure change is independent of flame thickness, linearly dependent on flame speed and linearly dependent on heat release ratio.

Flames of zero thickness

The special case of an infinitely thin flame is now developed. For a flame of zero thickness the flow field variables can be modelled using a Heaviside function,

$$\rho = (\rho_u - \rho_b)H(\zeta_f - |\zeta|) + \rho_b, \quad (8)$$
$$Y = H(\zeta_f - |\zeta|).$$

Substituting these functions into the species transport equation and integrating across the flame,

$$\int_0^{\zeta^+}\dot{\omega}d\zeta = \rho_u V_f(\tau)H(\zeta_f) \quad (9)$$

where V_f is the flame propagation velocity

$$V_f(\tau) = -\frac{d\zeta_f}{d\tau}. \quad (10)$$
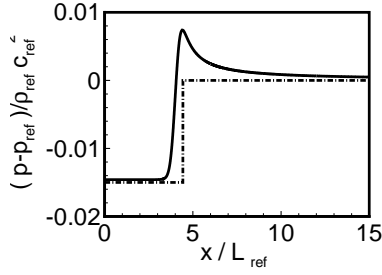
Figure 6: Non-dimensional pressure $(p - p_{ref})/\rho_{ref} c_{ref}^2$ from i) DNS, solid line, ii) zero flame thickness, dash-dot.

Therefore, for a flame of zero thickness the solution can be expressed using a Heaviside function

$$p'(x,t) = \rho_u c_b \left(1 - \frac{T_u}{T_b} \right) S_L \times$$
$$H(t - |x|/c_b) \left(\frac{V_f(\tau)}{S_L} H(\zeta_f(\tau)) - 1 \right) \Big|_{\tau = t - |x|/c_b}. \quad (11)$$

Equation 11 shows that the steady state far-field pressure (*i.e.* as $t \longrightarrow \infty$) is the same as that obtained from the earlier theoretical analysis for finite flame thickness.

Flames of zero thickness propagating at S_L

Assuming a constant propagation velocity $V_f = S_L$, the flame position can be described as

$$\zeta_f = \zeta_0 - S_L \tau, \quad (12)$$

where ζ_0 is the initial position of the flame. Therefore the solution of the wave equation can be obtained from equation 11

$$p'(x,t) = -\rho_u c_b \left(1 - \frac{T_u}{T_b} \right) S_L \times$$
$$H(t - |x|/c_b) H \left[S_L \left(t - \frac{|x|}{c_b} \right) - \zeta_0 \right]. \quad (13)$$

Equation 13 features a Heaviside function $H(x,t)$ travelling at the speed of sound in the burned gas. The steady state far-field pressure in equation 13 can be rearranged in a non-dimensional form as a function of temperature ratio and laminar flame speed

$$\frac{p'}{\rho_u c_u^2} = -\frac{S_L}{c_u} \left(1 - \frac{T_u}{T_b} \right) \sqrt{\frac{T_b}{T_u}}. \quad (14)$$

Figure 6 compares the zero flame thickness results with DNS (equation 13). The graph shows the pressure versus x at some instant after annihilation. The predicted step change in the pressure agrees with the numerical results.

Conclusions

This paper presented a numerical and theoretical study of sound production by planar premixed flame annihilation events. Direct Numerical Simulations (DNS) using a higher order accurate solver that was appropriate for aeroacoustic studies was first used to examine sound production and propagation by these events. The simulations showed that annihilation events could be a significant source of sound, which was consistent with previously reported studies. The far-field sound was compared for different flame thicknesses. It was found that there was relatively little influence of flame thickness.

A theory was then presented that related the far-field sound to the flame annihilation by using Dowling's [4] extended form of Lighthill's acoustic analogy. This theory retained only the heat release source term from Lighthill's equation, and agreed closely with the corresponding numerical results. From these more general theoretical results, increasingly restrictive assumptions were then applied. The assumption of an infinitely thin flame propagating at constant velocity was demonstrated to be adequate for prediction of the the steady state pressure change only.

References

[1] Candel, S., Durox, D., Ducruix, S., Birbaud, A. L., Noiray, N. and Schuller, T., Flame dynamics and combustion noise: progress and challenges, *International Journal of Aeroacoustics*, **8**, 2009, 1–56.

[2] Candel, S., Durox, D. and Schuller, T., Flame interactions as a source of noise and combustion instabilities, in *Collection of Technical Papers-10th AIAA/CEAS Aeroacoustics Conference*, 2004.

[3] Cuenot, B., Bedet, B. and Corjon, A., *NTMIX3D user's guide manual, Preliminary Version 1.0*, 1997.

[4] Dowling, A. P., *Modern Methods in Analytical Acoustics*, Springer, 1992 378–403.

[5] Duffy, D. G., *Green's Functions with Applications*, Chapman & Hall/CRC, 2001.

[6] Kidin, N., Librovicht, V., Robertst, J. and Vuillermoz, M., On sound sources in turbulent combustion, *Dynamics of flames and reactive systems*, 343–355.

[7] Lieuwen, T., Modeling premixed combustion-acoustic wave interactions: A review, *J. Propulsion Power*, **19**, 2003, 765–781.

[8] Lighthill, M. J., On sound generation aerodynamically I. General Theory, *Proc. of the Royal Soc. of London*, **211**, 1951, 564–587.

[9] Poinsot, T. J. and Lele, S. K., Boundary conditions for direct simulations of compressible viscous flows, *Journal of Computational Physics*, **101**, 1992, 104–129.

[10] Strahle, W. C., On combustion generated noise, *Journal of Fluid Mechanics*, **49**, 1971, 399–414.

[11] Strahle, W. C., Combustion noise, *Progress in Energy and Combustion Science*, **4**, 1978, 157–176.